Transverse single-spin asymmetries in proton-proton collisions at the AFTER@LHC experiment in a TMD factorisation scheme

M. Anselmino,[1,2] U. D'Alesio,[3,4] and S. Melis[1]

[1] *Dipartimento di Fisica, Università di Torino, Via P. Giuria 1, I-10125 Torino, Italy*
[2] *INFN, Sezione di Torino, Via P. Giuria 1, I-10125 Torino, Italy*
[3] *Dipartimento di Fisica, Università di Cagliari, Cittadella Universitaria, I-09042 Monserrato (CA), Italy*
[4] *INFN, Sezione di Cagliari, C.P. 170, I-09042 Monserrato (CA), Italy*

(Dated: December 14, 2015)

The inclusive large-p_T production of a single pion, jet or direct photon, and Drell-Yan processes, are considered for proton-proton collisions in the kinematical range expected for the fixed-target experiment AFTER, proposed at LHC. For all these processes, predictions are given for the transverse single-spin asymmetry, A_N, computed according to a Generalised Parton Model previously discussed in the literature and based on TMD factorisation. Comparisons with the results of a collinear twist-3 approach, recently presented, are made and discussed.

PACS numbers: 13.88.+e, 13.85.Ni, 13.85.Qk

I. INTRODUCTION AND FORMALISM

Transverse Single-Spin Asymmetries (TSSAs), have been abundantly observed in several inclusive proton-proton experiments since a long time; when reaching large enough energies and p_T values, their understanding from basic quark-gluon QCD interactions is a difficult and fascinating task, which has always been one of the major challenges for QCD.

In fact, large TSSAs cannot be generated by the hard elementary processes, because of helicity conservation (in the massless limit) typical of QED and QCD interactions; indeed, such asymmetries were expected to vanish at high energies. Their persisting must be related to non perturbative properties of the nucleon structure, such as parton intrinsic and orbital motion. A true understanding of the origin of TSSAs would allow a deeper understanding of the nucleon structure.

Since the 1990s two different, although somewhat related, approaches have attempted to tackle the problem. One is based on the collinear QCD factorisation scheme and involves as basic quantities, which can generate single spin dependences, higher- twist quark-gluon-quark correlations in the nucleon as well as higher-twist fragmentation correlators. The second approach is based on a physical, although unproven, generalisation of the parton model, with the inclusion, in the factorisation scheme, of transverse momentum dependent partonic distribution and fragmentation functions (TMDs), which also can generate single spin dependences. The twist-3 correlations are related to moments of some TMDs. We refer to Refs. [1–9], and references therein, for a more detailed account of the two approaches, and possible variations, with all relevant citations. Following Ref. [10], we denote by CT-3 the first approach while the second one is, as usual, denoted by GPM.

In this paper we consider TSSAs at the proposed AFTER@LHC experiment, in which high-energy protons extracted from the LHC beam would collide on a (polarised) fixed target of protons, with high luminosity. For a description of the physics potentiality of this experiment see Ref. [11] and for the latest technical details and importance for TMD studies see, for example, Ref. [12]. Due to its features the AFTER@LHC is an ideal experiment to study and understand the origin of SSAs and, in general, the role of QCD interactions in high-energy hadronic collisions; AFTER@LHC would be a polarised fixed target experiment with unprecedented high luminosity.

We recall our formalism by considering the Transverse Single-Spin Asymmetry A_N, measured in $p\,p^\uparrow \to h\,X$ inclusive reactions and defined as:

$$A_N = \frac{d\sigma^\uparrow - d\sigma^\downarrow}{d\sigma^\uparrow + d\sigma^\downarrow} \qquad \text{with} \qquad d\sigma^{\uparrow,\downarrow} \equiv \frac{E_h\, d\sigma^{p\,p^{\uparrow,\downarrow}\to h\,X}}{d^3\boldsymbol{p}_h}\,, \tag{1}$$

where $\uparrow,\downarrow$ are opposite spin orientations perpendicular to the x-z scattering plane, in the $p\,p^\uparrow$ c.m. frame. We define the $\uparrow$ direction as the $+\hat{y}$-axis and the unpolarised proton is moving along the $+\hat{z}$-direction. In such a process the only large scale is the transverse momentum $p_T = |(\boldsymbol{p}_h)_x|$ of the final hadron.

In the GPM A_N originates mainly from two spin and transverse momentum effects, one introduced by Sivers in the partonic distributions [13, 14], and one by Collins in the parton fragmentation process [15], being all the other effects strongly suppressed by azimuthal phase integrations [16]. According to the Sivers effect the number density of unpolarised quarks q (or gluons) with intrinsic transverse momentum $\boldsymbol{k}_\perp$ inside a transversely polarised proton $p^\uparrow$,

with three-momentum $\boldsymbol{P}$ and spin polarisation vector $\boldsymbol{S}$, can be written as

$$\hat{f}_{q/p^\uparrow}(x,\boldsymbol{k}_\perp) = f_{q/p}(x,k_\perp) + \frac{1}{2}\,\Delta^N f_{q/p^\uparrow}(x,k_\perp)\;\boldsymbol{S}\cdot(\hat{\boldsymbol{P}}\times\hat{\boldsymbol{k}}_\perp)\,, \tag{2}$$

where x is the proton light-cone momentum fraction carried by the quark, $f_{q/p}(x,k_\perp)$ is the unpolarised TMD ($k_\perp = |\boldsymbol{k}_\perp|$) and $\Delta^N f_{q/p^\uparrow}(x,k_\perp)$ is the Sivers function. $\hat{\boldsymbol{P}} = \boldsymbol{P}/|\boldsymbol{P}|$ and $\hat{\boldsymbol{k}}_\perp = \boldsymbol{k}_\perp/k_\perp$ are unit vectors. Notice that the Sivers function is most often denoted as $f_{1T}^{\perp q}(x,k_\perp)$ [17]; this notation is related to ours by [18]

$$\Delta^N f_{q/p^\uparrow}(x,k_\perp) = -\frac{2\,k_\perp}{m_p}\,f_{1T}^{\perp q}(x,k_\perp)\,, \tag{3}$$

where m_p is the proton mass.

Similarly, according to the Collins effect the number density of unpolarised hadrons h with transverse momentum $\boldsymbol{p}_\perp$ resulting in the fragmentation of a transversely polarised quark $q^\uparrow$, with three-momentum $\boldsymbol{q}$ and spin polarisation vector $\boldsymbol{S}_q$, can be written as

$$\hat{D}_{q^\uparrow/h}(z,\boldsymbol{p}_\perp) = D_{h/q}(z,p_\perp) + \frac{1}{2}\,\Delta^N D_{q^\uparrow/h}(z,p_\perp)\;\boldsymbol{S}_q\cdot(\hat{\boldsymbol{q}}\times\hat{\boldsymbol{p}}_\perp)\,, \tag{4}$$

where z is the parton light-cone momentum fraction carried by the hadron, $D_{h/q}(z,p_\perp)$ is the unpolarised TMD ($p_\perp = |\boldsymbol{p}_\perp|$) and $\Delta^N D_{q^\uparrow/h}(z,p_\perp)$ is the Collins function. $\hat{\boldsymbol{q}} = \boldsymbol{q}/|\boldsymbol{q}|$ and $\hat{\boldsymbol{p}}_\perp = \boldsymbol{p}_\perp/p_\perp$ are unit vectors. Notice that the Collins function is most often denoted as $H_1^{\perp q}(z,p_\perp)$ [17]; this notation is related to ours by [18]

$$\Delta^N D_{h/q^\uparrow}(z,p_\perp) = \frac{2\,p_\perp}{z M_h}\,H_1^{\perp q}(z,p_\perp)\,, \tag{5}$$

where M_h is the hadron mass.

According to the GPM formalism [1, 2, 16], A_N can then be written as:

$$A_N = \frac{[d\sigma^\uparrow - d\sigma^\downarrow]_{\rm Sivers} + [d\sigma^\uparrow - d\sigma^\downarrow]_{\rm Collins}}{d\sigma^\uparrow + d\sigma^\downarrow}\;. \tag{6}$$

The Collins and Sivers contributions were recently studied, respectively in Refs. [1] and [2], and are given by:

$$\begin{aligned}[d\sigma^\uparrow - d\sigma^\downarrow]_{\rm Sivers} \;=& \sum_{a,b,c,d}\int \frac{dx_a\,dx_b\,dz}{16\,\pi^2\,x_a\,x_b\,z^2 s}\;d^2\boldsymbol{k}_{\perp a}\,d^2\boldsymbol{k}_{\perp b}\,d^3\boldsymbol{p}_\perp\,\delta(\boldsymbol{p}_\perp\cdot\hat{\boldsymbol{p}}_c)\,J(p_\perp)\,\delta(\hat{s}+\hat{t}+\hat{u})\\
&\times\;\Delta^N f_{a/p^\uparrow}(x_a,k_{\perp a})\,\cos(\phi_a)\,f_{b/p}(x_b,k_{\perp b})\,\frac{1}{2}\left[|\hat{M}_1^0|^2+|\hat{M}_2^0|^2+|\hat{M}_3^0|^2\right]_{ab\to cd}\,D_{h/c}(z,p_\perp)\,,
\end{aligned} \tag{7}$$

and

$$\begin{aligned}[d\sigma^\uparrow - d\sigma^\downarrow]_{\rm Collins} \;=& \sum_{q_a,b,q_c,d}\int \frac{dx_a\,dx_b\,dz}{16\,\pi^2\,x_a\,x_b\,z^2 s}\;d^2\boldsymbol{k}_{\perp a}\,d^2\boldsymbol{k}_{\perp b}\,d^3\boldsymbol{p}_\perp\,\delta(\boldsymbol{p}_\perp\cdot\hat{\boldsymbol{p}}_c)\,J(p_\perp)\,\delta(\hat{s}+\hat{t}+\hat{u})\\
&\times\;\Delta_T q_a(x_a,k_{\perp a})\,\cos(\phi_a+\varphi_1-\varphi_2+\phi_\pi^H)\\
&\times\;f_{b/p}(x_b,k_{\perp b})\,\left[\hat{M}_1^0\,\hat{M}_2^0\right]_{q_a b\to q_c d}\,\Delta^N D_{h/q_c^\uparrow}(z,p_\perp)\,.
\end{aligned} \tag{8}$$

For details and a full explanation of the notations in the above equations we refer to Ref. [16] (where $\boldsymbol{p}_\perp$ is denoted as $\boldsymbol{k}_{\perp C}$). It suffices to notice here that $J(p_\perp)$ is a kinematical factor, which at $\mathcal{O}(p_\perp/E_h)$ equals 1. The phase factor $\cos(\phi_a)$ in Eq. (7) originates directly from the $\boldsymbol{k}_\perp$ dependence of the Sivers distribution [$\boldsymbol{S}\cdot(\hat{\boldsymbol{P}}\times\hat{\boldsymbol{k}}_\perp)$, Eq. (2)]. The (suppressing) phase factor $\cos(\phi_a+\varphi_1-\varphi_2+\phi_\pi^H)$ in Eq. (8) originates from the $\boldsymbol{k}_\perp$ dependence of the unintegrated transversity distribution $\Delta_T q$, the polarized elementary interaction and the spin-$\boldsymbol{p}_\perp$ correlation in the Collins function. The explicit expressions of φ_1, φ_2 and ϕ_π^H in terms of the integration variables can be found via Eqs. (60)-(63) in [16] and Eqs. (35)-(42) in [19].

The $\hat{M}_i^0$'s are the three independent hard scattering helicity amplitudes describing the lowest order QCD interactions. The sum of their moduli squared is related to the elementary unpolarised cross section $d\hat{\sigma}^{ab\to cd}$, that is

$$\frac{d\hat{\sigma}^{ab\to cd}}{d\hat{t}} = \frac{1}{16\pi\hat{s}^2}\,\frac{1}{2}\sum_{i=1}^{3}|\hat{M}_i^0|^2\,. \tag{9}$$

The explicit expressions of the combinations of $\hat{M}_i^0$'s which give the QCD dynamics in Eqs. (7) and (8), can be found, for all possible elementary interactions, in Ref. [16] (see also Ref. [1] for a correction to one of the product of amplitudes). The QCD scale is chosen as $Q = p_T$.

The denominator of Eq. (1) or (6) is twice the unpolarised cross section and is given in our TMD factorisation by the same expression as in Eq. (7), where one simply replaces the factor $\Delta^N f_{a/p^\uparrow} \cos(\phi_a)$ with $2 f_{a/p}$.

II. A_N FOR SINGLE PION, JET AND DIRECT PHOTON PRODUCTION

We present here our results for A_N, Eq. (1), based on our GPM scheme, Eqs. (6), (7) and (8). The TMDs which enter in these equations are those extracted from the analysis of Semi Inclusive Deep Inelastic (SIDIS) and e^+e^- data [20–23], adopting simple factorised forms, which we recall here. For the unpolarised TMD partonic distributions and fragmentation functions we have, respectively:

$$f_{q/p}(x,k_\perp) = f_{q/p}(x)\,\frac{e^{-k_\perp^2/\langle k_\perp^2\rangle}}{\pi\langle k_\perp^2\rangle} \qquad \langle k_\perp^2\rangle = 0.25\,\mathrm{GeV}^2 \tag{10}$$

and

$$D_{h/q}(z,p_\perp) = D_{h/q}(z)\,\frac{e^{-p_\perp^2/\langle p_\perp^2\rangle}}{\pi\langle p_\perp^2\rangle} \qquad \langle p_\perp^2\rangle = 0.20\,\mathrm{GeV}^2\,. \tag{11}$$

The Sivers function is parameterised as

$$\Delta^N f_{q/p^\uparrow}(x,k_\perp) = 2\,\mathcal{N}_q^S(x)\,f_{q/p}(x)\,h(k_\perp)\,\frac{e^{-k_\perp^2/\langle k_\perp^2\rangle}}{\pi\langle k_\perp^2\rangle}\,, \tag{12}$$

where

$$\mathcal{N}_q^S(x) = N_q^S x^{\alpha_q}(1-x)^{\beta_q}\,\frac{(\alpha_q+\beta_q)^{(\alpha_q+\beta_q)}}{\alpha_q^{\alpha_q}\beta_q^{\beta_q}}\,, \tag{13}$$

with $|N_q^S| \le 1$, and

$$h(k_\perp) = \sqrt{2e}\,\frac{k_\perp}{M}\,e^{-k_\perp^2/M^2}\,. \tag{14}$$

Similarly, the quark transversity distribution, $\Delta_T q(x,k_\perp)$, and the Collins fragmentation function, $\Delta^N D_{h/q^\uparrow}(z,p_\perp)$, have been parametrized as follows:

$$\Delta_T q(x,k_\perp) = \frac{1}{2}\,\mathcal{N}_q^T(x)\,\left[\,f_{q/p}(x) + \Delta q(x)\,\right]\,\frac{e^{-k_\perp^2/\langle k_\perp^2\rangle}}{\pi\langle k_\perp^2\rangle}\,, \tag{15}$$

$$\Delta^N D_{h/q^\uparrow}(z,p_\perp) = 2\mathcal{N}_q^C(z)\,D_{h/q}(z)\,h(p_\perp)\,\frac{e^{-p_\perp^2/\langle p_\perp^2\rangle}}{\pi\langle p_\perp^2\rangle}\,, \tag{16}$$

where $\Delta q(x)$ is the usual collinear quark helicity distribution,

$$\mathcal{N}_q^T(x) = N_q^T x^{a_q}(1-x)^{b_q}\,\frac{(a_q+b_q)^{(a_q+b_q)}}{a_q^{a_q}a_q^{b_q}}\,, \tag{17}$$

$$\mathcal{N}_q^C(z) = N_q^C z^{\gamma_q}(1-z)^{\delta_q}\,\frac{(\gamma_q+\delta_q)^{(\gamma_q+\delta_q)}}{\gamma_q^{\gamma_q}\delta_q^{\delta_q}}\,, \tag{18}$$

with $|N_q^{T(C)}| \le 1$, and

$$h(p_\perp) = \sqrt{2e}\,\frac{p_\perp}{M_c}\,e^{-p_\perp^2/M_c^2}\,. \tag{19}$$

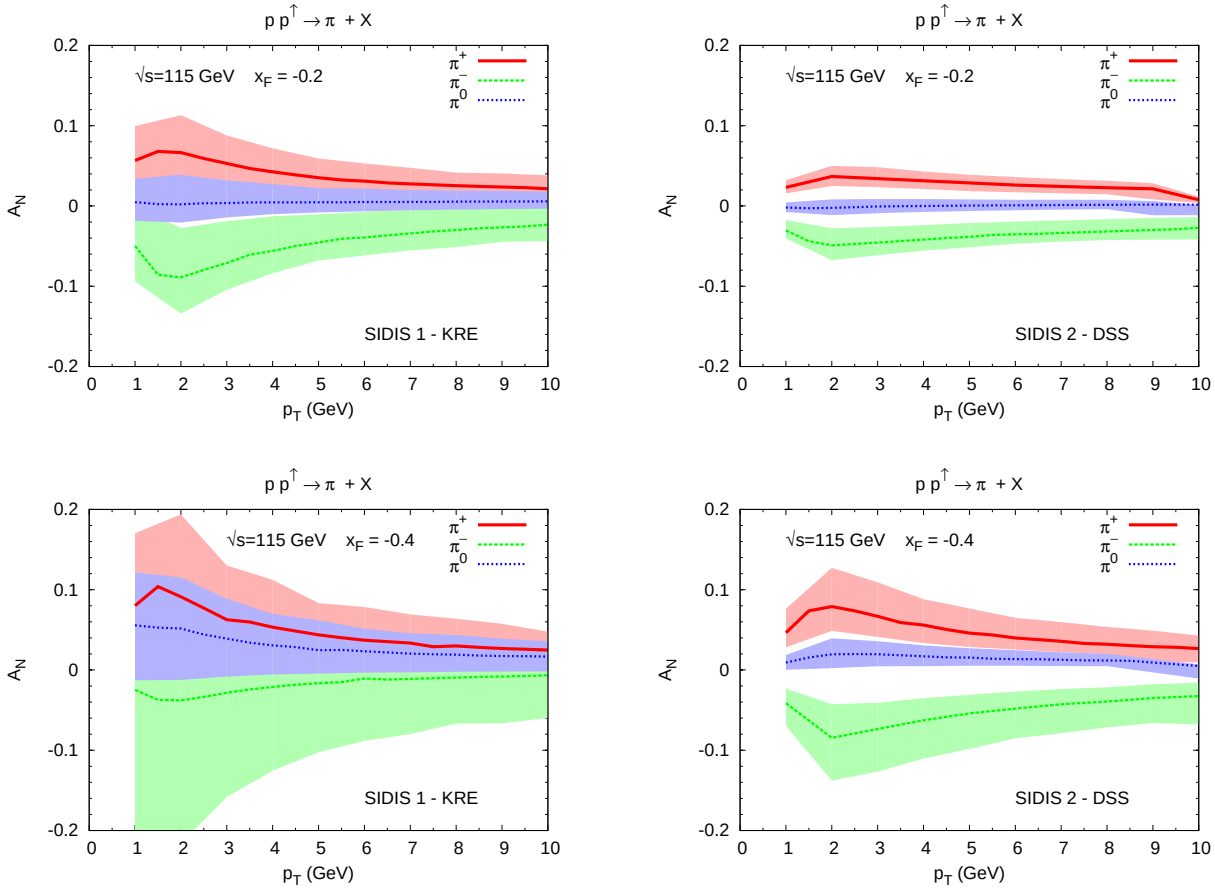

FIG. 1: Our theoretical estimates for A_N vs. p_T at $\sqrt{s} = 115$ GeV, $x_F = -0.2$ (upper plots) and $x_F = -0.4$ (lower plots) for inclusive $\pi^\pm$ and π^0 production in $p p^\uparrow \to \pi X$ processes, computed according to Eqs (6)–(8) of the text. The contributions from the Sivers and the Collins effects are added together. The computation is performed adopting the Sivers and Collins functions of Refs. [20, 22] (SIDIS 1 - KRE, left panels), and of Refs. [21, 23] (SIDIS 2 - DSS, right panels). The overall statistical uncertainty band, also shown, is the envelope of the two independent statistical uncertainty bands obtained following the procedure described in Appendix A of Ref. [21].

All details concerning the motivations for such a choice, the values of the parameters and their derivation can be found in Refs. [20–23]. We do not repeat them here, but in the caption of each figure we will give the corresponding references which allow to fix all necessary values.

We present our results on A_N for the process $p p^\uparrow \to \pi X$ at the expected AFTER@LHC energy ($\sqrt{s} = 115$ GeV) in Figs. 1-3. Following Refs. [1, 2], our results are given for two possible choices of the SIDIS TMDs, and are shown as function of p_T at two fixed x_F values (Fig. 1), as function of x_F at two fixed rapidity y values (Fig. 2) and as function of rapidity at one fixed p_T value (Fig. 3). x_F is the usual Feynman variable defined as $x_F = 2p_L/\sqrt{s}$ where $p_L = (\boldsymbol{p}_h)_z$ is the z-component of the final hadron momentum. Notice that, in our chosen reference frame, a forward production, with respect to the polarised proton, means negative values of x_F. The uncertainty bands reflects the uncertainty in the determinations of the TMDs and are computed according to the procedure explained in the Appendix of Ref. [21]. More information can be found in the figure captions.

Notice that, for both our choices of the Sivers functions, the gluon Sivers distributions are taken to be vanishing, as suggested by data [21, 24]. Gluon channels contribute instead to the unpolarised cross sections, in the denominator of Eq. (1) or (6). For the unpolarised partonic distributions we adopt the GRV98LO PDF set [25] and for the fragmentation functions the DSS set from Ref. [26] and the Kretzer (KRE) set from Ref. [27].

The analogous results for the single direct photon are shown in Figs. 4-6 (where $x_F = 2(\boldsymbol{p}_{\rm jet})_z/\sqrt{s}$), and those for the single jet production in Figs. 7-9 ($x_F = 2(\boldsymbol{p}_\gamma)_z/\sqrt{s}$). In these cases, obviously, there is no fragmentation process and only the Sivers effect contributes to A_N, with $D_{h/c}(z, p_\perp)$ simply replaced by $\delta(z-1)\,\delta^2(\boldsymbol{p}_\perp)$ in Eq. (7) (see Ref. [2] for further details). In our leading order treatment the jet coincides with a single final parton. Notice that for

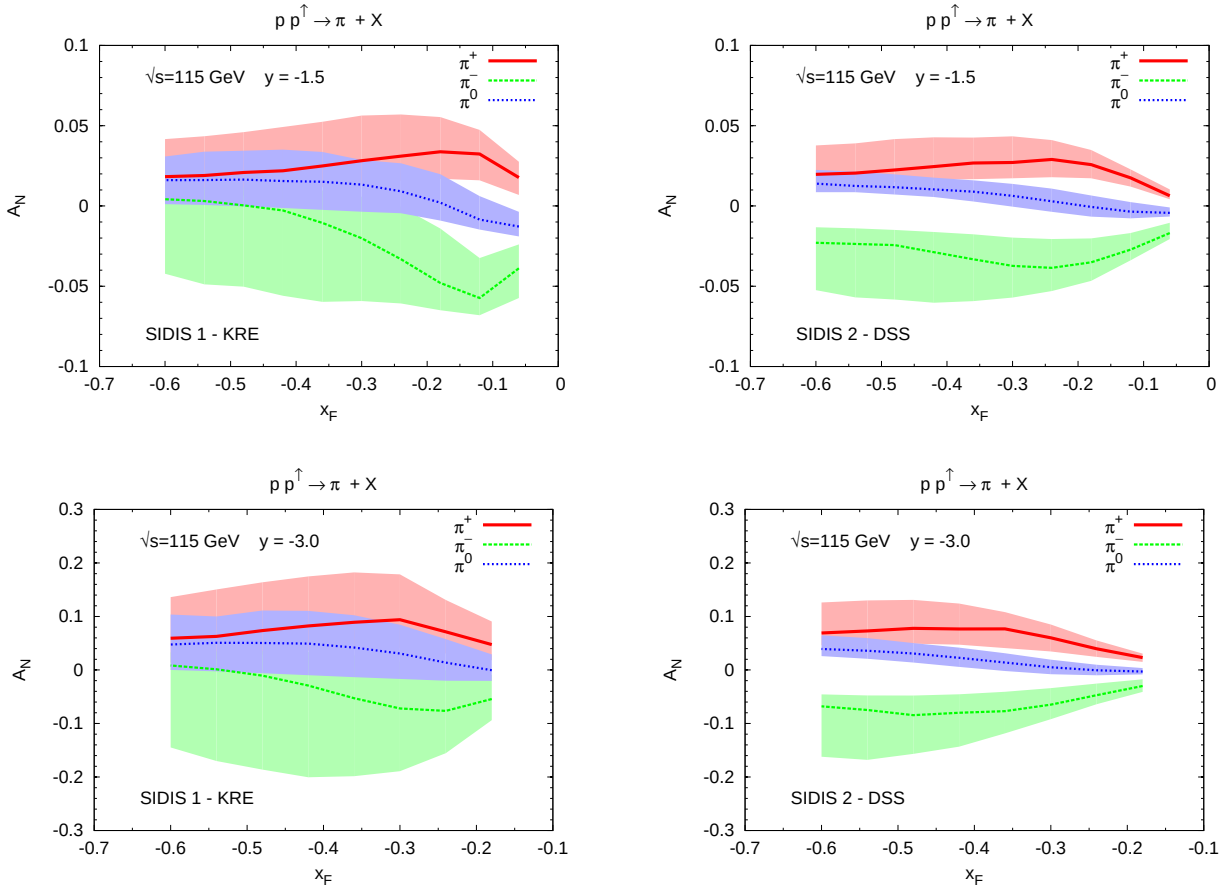

FIG. 2: Our theoretical estimates for A_N vs. x_F at $\sqrt{s} = 115$ GeV, $y = -1.5$ (upper plots) and $y = -3.0$ (lower plots) for inclusive $\pi^\pm$ and π^0 production in $p\,p^\uparrow \to \pi\,X$ processes, computed according to Eqs (6)–(8) of the text. The contributions from the Sivers and the Collins effects are added together. The computation is performed adopting the Sivers and Collins functions of Refs. [20, 22] (SIDIS 1 - KRE, left panels), and of Refs. [21, 23] (SIDIS 2 - DSS, right panels). The overall statistical uncertainty band, also shown, is the envelope of the two independent statistical uncertainty bands obtained following the procedure described in Appendix A of Ref. [21].

a jet production we have all the same QCD subprocesses which contribute to hadron production, while for a direct photon production the basic partonic subprocesses are the Compton scattering $g\,q(\bar{q}) \to \gamma\,q(\bar{q})$ and the annihilation process $q\,\bar{q} \to \gamma\,g$ [28].

III. A_N FOR DRELL-YAN PROCESSES

Drell-Yan (D-Y) processes are expected to play a crucial role in our understanding of the origin, at the partonic level, of TSSAs. For such processes, like for SIDIS processes and contrary to single hadron production, the TMD factorisation has been proven to hold, so that there is a general consensus that the Sivers effect should be visible via TSSAs in D-Y [29–32]. Not only: the widely accepted interpretation of the QCD origin of TSSAs as final or initial state interactions of the scattering partons [33] leads to the conclusion that the Sivers function has opposite signs in SIDIS and D-Y processes [34]. Which remains to be seen.

Predictions for Sivers A_N in D-Y and at different possible experiments were given in Ref. [35], which we follow here.

In Ref. [35] predictions were given for the $p^\uparrow p \to \ell^+\ell^- X$ D-Y process in the $p^\uparrow - p$ c.m. frame, in which one observes the four-momentum q of the final $\ell^+\ell^-$ pair. Notice that $q^2 = M^2$ is the large scale in the process, while $q_T = |\boldsymbol{q}_T|$ is the small one. In order to collect data at all azimuthal angles, one defines the weighted spin asymmetry:

$$A_N^{\sin(\phi_\gamma - \phi_S)} \equiv \frac{\int_0^{2\pi} d\phi_\gamma \,[d\sigma^\uparrow - d\sigma^\downarrow]\,\sin(\phi_\gamma - \phi_S)}{\frac{1}{2}\int_0^{2\pi} d\phi_\gamma \,[d\sigma^\uparrow + d\sigma^\downarrow]} \tag{20}$$

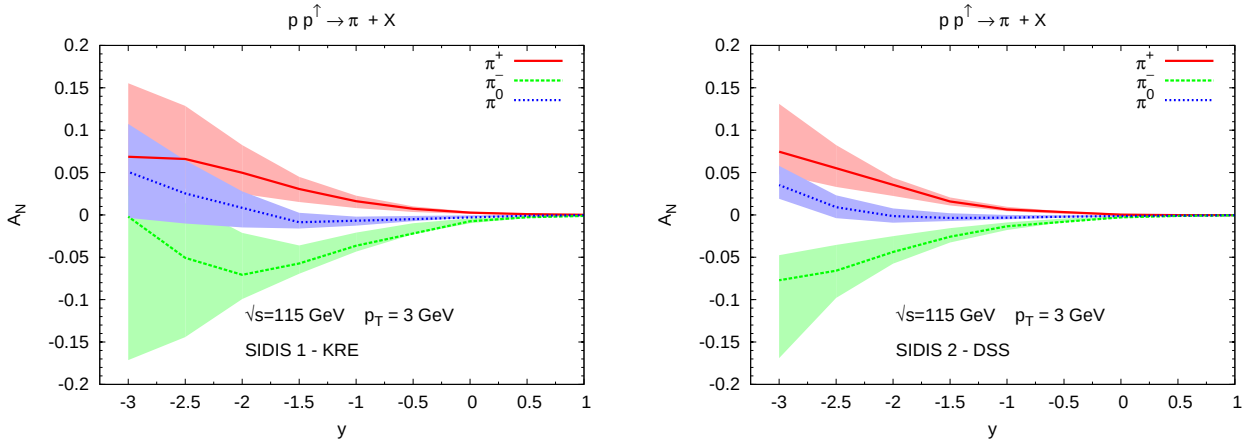

FIG. 3: Our theoretical estimates for A_N vs. y at $\sqrt{s} = 115$ GeV and $p_T = 3$ GeV, for inclusive $\pi^\pm$ and π^0 production in $p\,p^\uparrow \to \pi\, X$ processes, computed according to Eqs (6)–(8) of the text. The contributions from the Sivers and the Collins effects are added together. The computation is performed adopting the Sivers and Collins functions of Refs. [20, 22] (SIDIS 1 - KRE, left panel), and of Refs. [21, 23] (SIDIS 2 - DSS, right panel). The overall statistical uncertainty band, also shown, is the envelope of the two independent statistical uncertainty bands obtained following the procedure described in Appendix A of Ref. [21].

$$= \frac{\int d\phi_\gamma \left[\sum_q e_q^2 \int d^2\boldsymbol{k}_{\perp 1}\, d^2\boldsymbol{k}_{\perp 2}\, \delta^2(\boldsymbol{k}_{\perp 1} + \boldsymbol{k}_{\perp 2} - \boldsymbol{q}_T)\, \Delta^N f_{q/p^\uparrow}(x_1, \boldsymbol{k}_{\perp 1})\, f_{\bar{q}/p}(x_2, k_{\perp 2})\right] \sin(\phi_\gamma - \phi_S)}{\int d\phi_\gamma \left[\sum_q e_q^2 \int d^2\boldsymbol{k}_{\perp 1}\, d^2\boldsymbol{k}_{\perp 2}\, \delta^2(\boldsymbol{k}_{\perp 1} + \boldsymbol{k}_{\perp 2} - \boldsymbol{q}_T)\, f_{q/p}(x_1, k_{\perp 1})\, f_{\bar{q}/p}(x_2, k_{\perp 2})\right]}\,, \qquad (21)$$

where ϕ_γ and ϕ_S are respectively the azimuthal angle of the $\ell^+\ell^-$ pair and of the proton transverse spin and we have defined (see Eq. (2)):

$$\Delta^N f_{q/p^\uparrow}(x, \boldsymbol{k}_\perp) \equiv \Delta^N f_{q/p^\uparrow}(x, k_\perp)\, \boldsymbol{S} \cdot (\hat{\boldsymbol{P}} \times \hat{\boldsymbol{k}}_\perp) = \hat{f}_{q/p^\uparrow}(x, \boldsymbol{k}_\perp) - \hat{f}_{q/p^\downarrow}(x, \boldsymbol{k}_\perp)\,. \qquad (22)$$

Adopting for the unpolarised TMD and the Sivers function the same expressions as in Eqs. (10) and (12)-(14) allows, at $\mathcal{O}(k_\perp/M)$, an analytical integration of the numerator and denominator of Eq. (21), resulting in a simple expression for the asymmetry $A_N^{\sin(\phi_\gamma - \phi_S)}$ [35].

Notice that we consider here the $p\,p^\uparrow \to \ell^+\ell^- X$ D-Y process in the $p - p^\uparrow$ c.m. frame. For such a process the TSSA is given by [35]

$$A_N^{\sin(\phi_\gamma - \phi_S)}(p\,p^\uparrow \to \gamma^* X;\, x_F, M, q_T) = -A_N^{\sin(\phi_\gamma - \phi_S)}(p^\uparrow\, p \to \gamma^* X;\, -x_F, M, q_T)\,. \qquad (23)$$

Our results for the Sivers asymmetry $A_N^{\sin(\phi_\gamma - \phi_S)}$ at AFTER@LHC, obtained following Ref. [35], Eq. (23) and using the SIDIS extracted Sivers function *reversed in sign*, are shown in Fig. 10. Further details can be found in the captions of these figures.

IV. COMMENTS AND CONCLUSIONS

Some final comments and further details might help in understanding the importance of the measurements of the TSSAs at AFTER@LHC.

- Most predictions given show clear asymmetries, sufficiently large as to be easily measurable, given the expected performance of AFTER@LHC [11]. The uncertainty bands reflects the uncertainty in the extraction of the Sivers and transversity functions from SIDIS data, which are focused on small and intermediate x values ($x \lesssim 0.3$); in fact the bands grow larger at larger values of $|x_F|$.

- The values of A_N found for pion production can be as large as 10% for $\pi^\pm$, while they are smaller for π^0. They result from the sum of the Sivers and the Collins effects. The relative importance of the two contributions varies according to the kinematical regions and the set of distributions and fragmentation functions adopted. As a

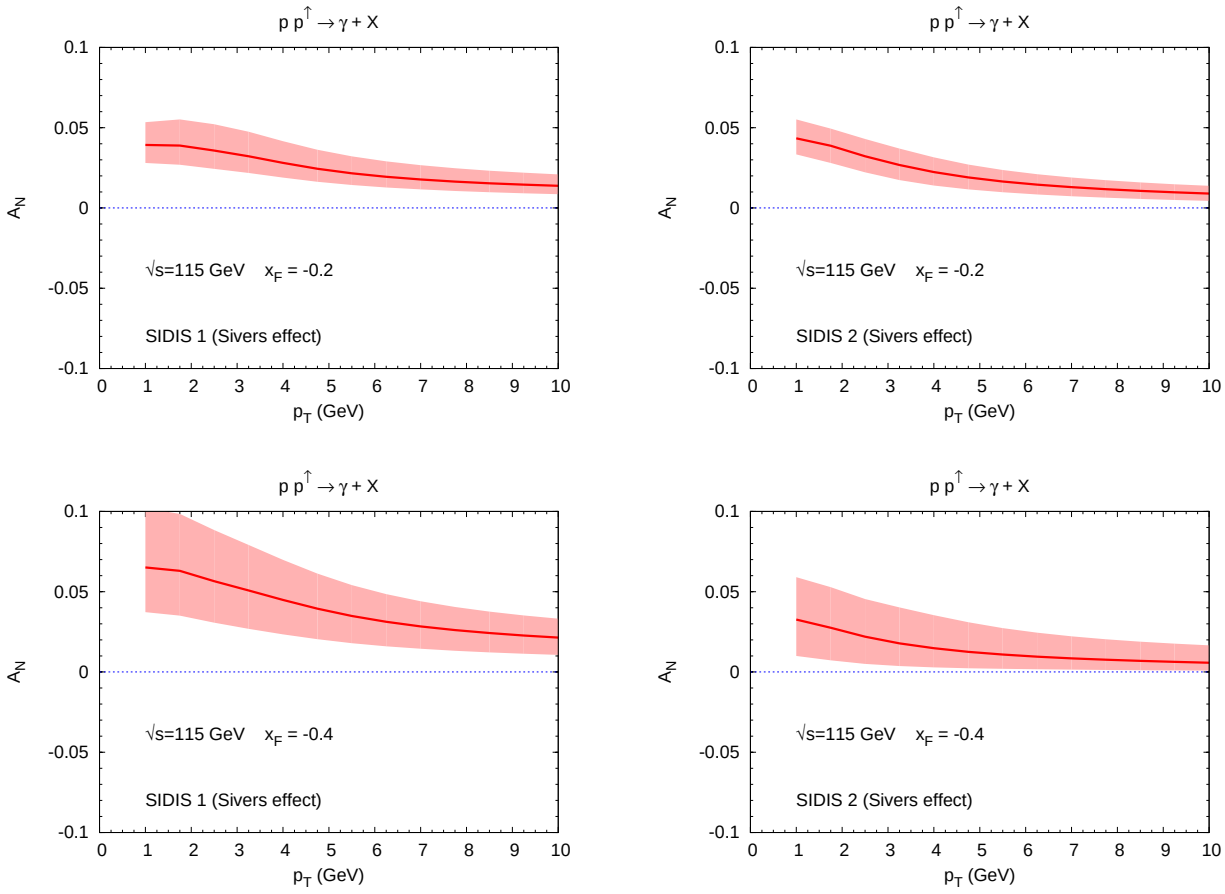

FIG. 4: Our theoretical estimates for A_N vs. p_T at $\sqrt{s} = 115$ GeV, $x_F = -0.2$ (upper plots) and $x_F = -0.4$ (lower plots) for inclusive photon production in $p\,p^\uparrow \to \gamma\,X$ processes, computed according to Eqs (6) and (7) of the text. Only the Sivers effect contributes. The computation is performed adopting the Sivers functions of Ref. [20] (SIDIS 1, left panels) and of Ref. [21] (SIDIS 2, right panels). The overall statistical uncertainty band, also shown, is obtained following the procedure described in Appendix A of Ref. [21].

tendency, the contribution from the Sivers effect is larger than the Collins contribution with the SIDIS 1 - KRE set, while the opposite is true for the SIDIS 2 - DSS set.

The values found here are in agreement, both in sign and qualitative magnitude, with the values found in Ref. [10] within the collinear twist-3 (CT-3) approach.

- The results for single photon production are interesting; they isolate the Sivers effect and our predictions show that they can reach values of about 5%, with a reduced uncertainty band. We find positive values of A_N as the relative weight of the quark charges leads to a dominance of the u quark and the Sivers functions $\Delta^N f_{u/p^\uparrow}$ is positive [20, 21].

  Our results, obtained within the GPM, have a similar magnitude as those obtained in Refs. [10] and [3], within the CT-3 approach, but have *an opposite sign*. Thus, a measurement of A_N for a single photon production, although difficult, would clearly discriminate between the two approaches.

- The values of A_N for single jet production, which might be interesting as they also have no contribution from the Collins effect, turn out to be very small and compatible with zero, due to a strong cancellation between the u and d quark contributions. The same result is found in Ref. [10].

- A measurement of $A_N^{\sin(\phi_\gamma - \phi_S)}$ in D-Y processes at AFTER@LHC is a most interesting one. In such a case the TMD factorisation has been shown to be valid and the Sivers asymmetry should show the expected sign change with respect to SIDIS processes [33, 34]. Our computations, Fig. 10, predict a clear asymmetry, which can be as sizeable as 10%, with a definite sign, even within the uncertainty band.

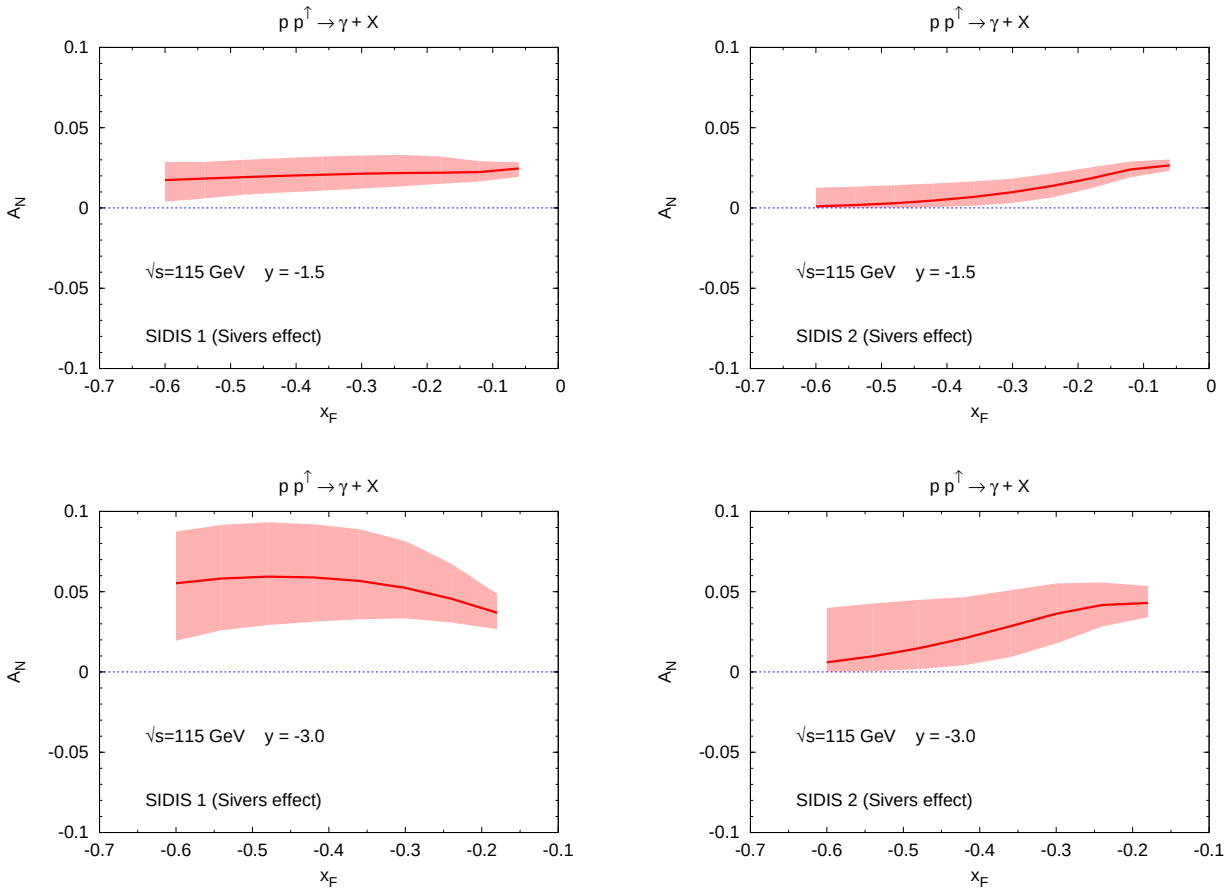

FIG. 5: Our theoretical estimates for A_N vs. x_F at $\sqrt{s} = 115$ GeV, $y = -1.5$ (upper plots) and $y = -3.0$ (lower plots) for inclusive photon production in $p\,p^\uparrow \to \gamma\,X$ processes, computed according to Eqs (6) and (7) of the text. Only the Sivers effect contributes. The computation is performed adopting the Sivers functions of Ref. [20] (SIDIS 1, left panels) and of Ref. [21] (SIDIS 2, right panels). The overall statistical uncertainty band, also shown, is obtained following the procedure described in Appendix A of Ref. [21].

Both the results of Ref. [10] and the results of this paper, obtain solid non negligible values for the TSSA A_N measurable at the AFTER@LHC experiment. The two sets of results are based on different approaches, respectively the CT-3 and the GPM factorisation schemes. While the magnitude of A_N is very similar in the two cases, the signs can be different; in particular, the TSSA for a direct photon production, $p\,p^\uparrow \to \gamma\,X$, has opposite signs in the two schemes.

In this paper we have also considered azimuthal asymmetries in polarised D-Y processes, related to the Sivers effect. As explained above, in this case, due to the presence of a large and a small scale, like in SIDIS, the TMD factorisation is valid, with the expectation of an opposite sign of the Sivers function in SIDIS and D-Y processes. Also this prediction can be checked at AFTER@LHC.

Acknowledgments

M.A. and S.M. acknowledge support from the "Progetto di Ricerca di Ateneo/CSP" (codice TO-Call3-2012-0103). U.D. is grateful to the Department of Theoretical Physics II of the Universidad Complutense of Madrid for the kind hospitality extended to him during the completion of this work.

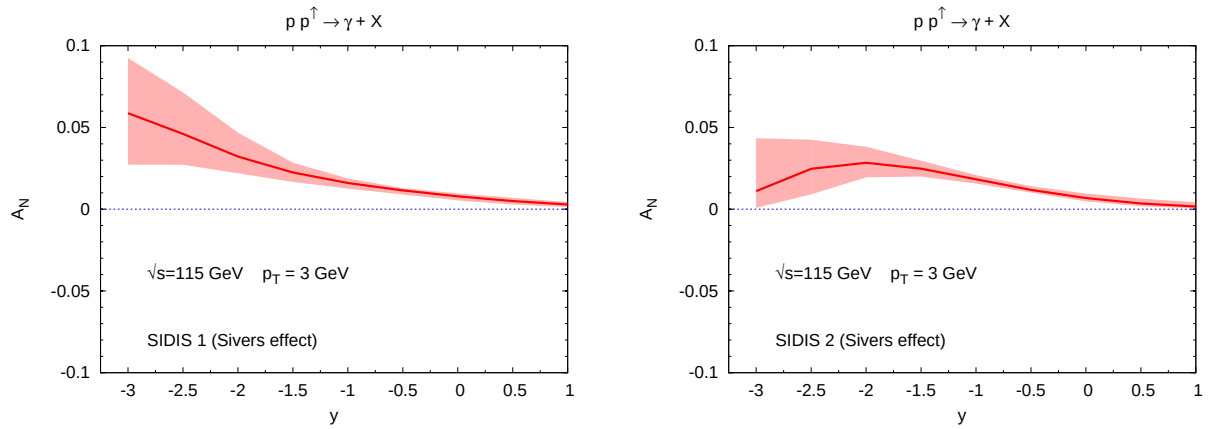

FIG. 6: Our theoretical estimates for A_N vs. y at $\sqrt{s} = 115$ GeV and $p_T = 3$ GeV, for inclusive photon production in $p\,p^\uparrow \to \gamma\,X$ processes, computed according to Eqs (6)–(8) of the text. Only the Sivers effects contributes. The computation is performed adopting the Sivers functions of Ref. [20] (SIDIS 1, left panel) and of Ref. [21] (SIDIS 2, right panel). The overall statistical uncertainty band, also shown, is the envelope of the two independent statistical uncertainty bands obtained following the procedure described in Appendix A of Ref. [21].

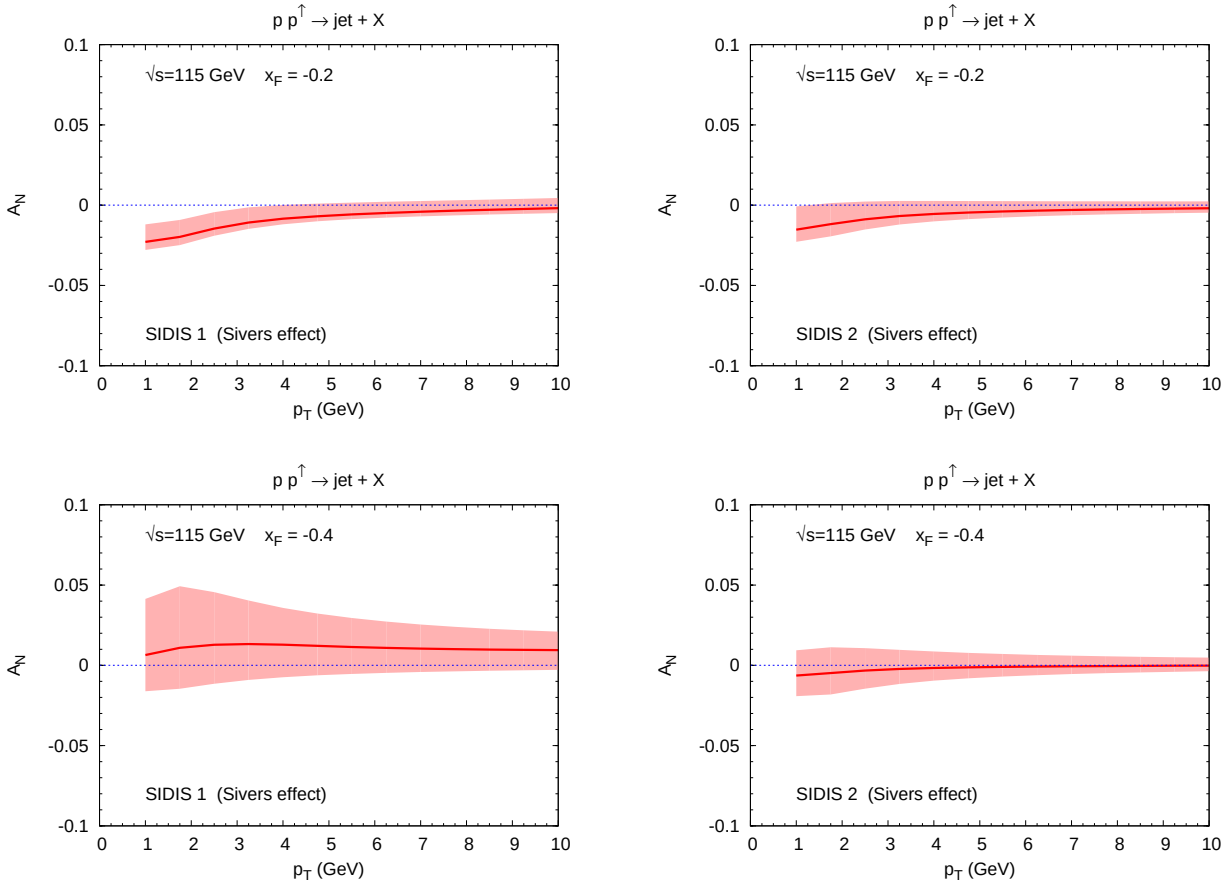

FIG. 7: Our theoretical estimates for A_N vs. x_F at $\sqrt{s} = 115$ GeV, $x_F = -0.2$ (upper plots) and $x_F = -0.4$ (lower plots) for inclusive single jet production in $p\,p^\uparrow \to \text{jet}\,X$ processes, computed according to Eqs (6) and (7) of the text. Only the Sivers effect contributes. The computation is performed adopting the Sivers functions of Ref. [20] (SIDIS 1, left panels) and of Ref. [21] (SIDIS 2, right panels). The overall statistical uncertainty band, also shown, is obtained following the procedure described in Appendix A of Ref. [21].

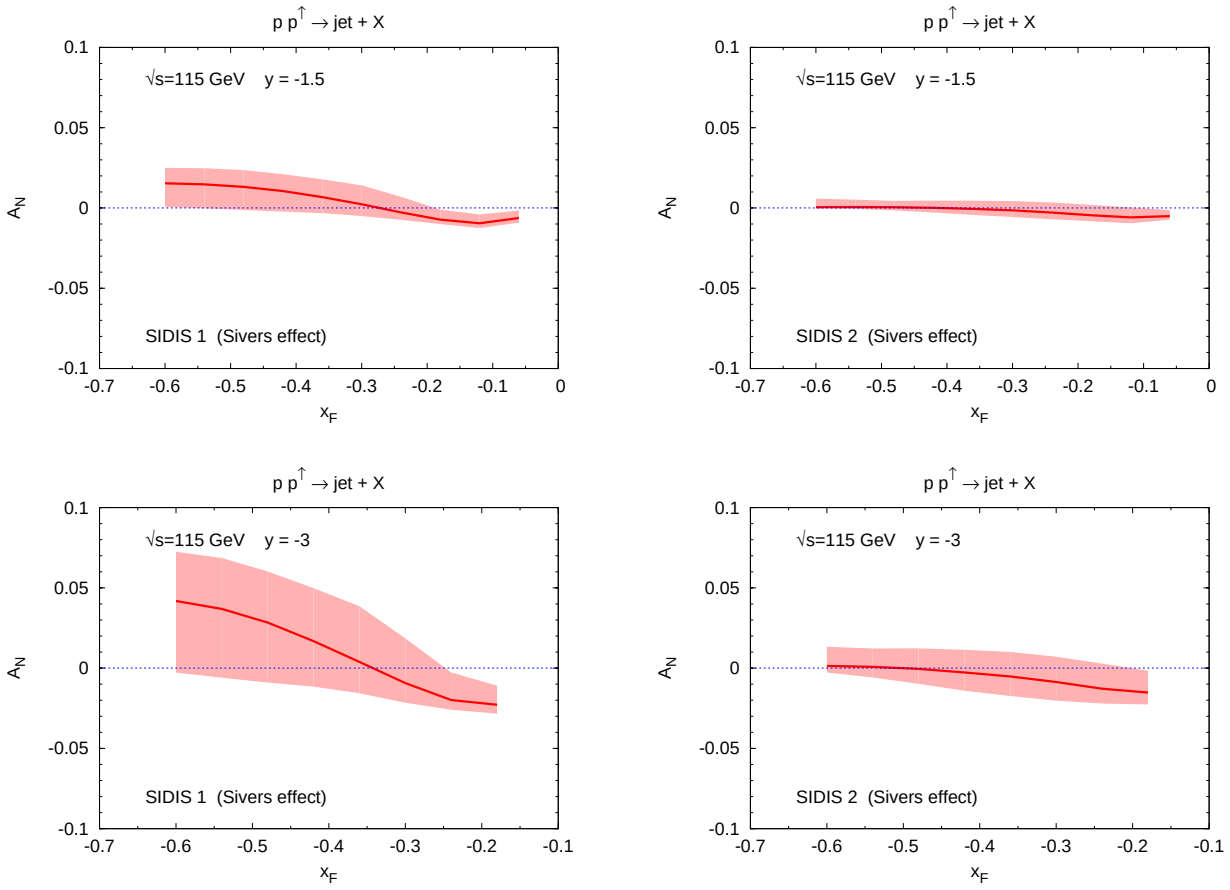

FIG. 8: Our theoretical estimates for A_N vs. x_F at $\sqrt{s} = 115$ GeV, $y = -1.5$ (upper plots) and $y = -3.0$ (lower plots) for inclusive single jet production in $pp^\uparrow \to \text{jet}\, X$ processes, computed according to Eqs (6) and (7) of the text. Only the Sivers effect contributes. The computation is performed adopting the Sivers functions of Ref. [20] (SIDIS 1, left panels) and of Ref. [21] (SIDIS 2, right panels). The overall statistical uncertainty band, also shown, is obtained following the procedure described in Appendix A of Ref. [21].

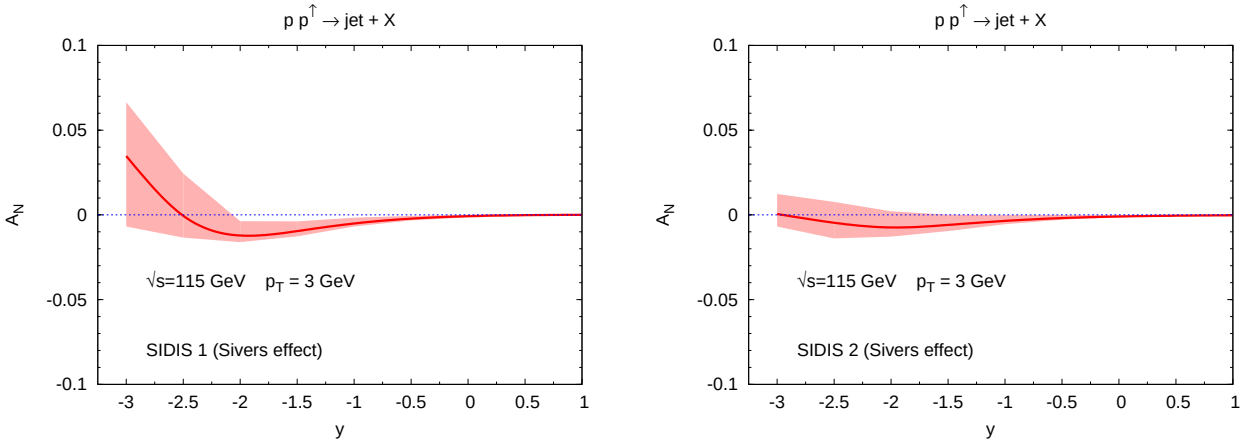

FIG. 9: Our theoretical estimates for A_N vs. y at $\sqrt{s} = 115$ GeV and $p_T = 3$ GeV, for inclusive single jet production in $pp^\uparrow \to \text{jet}\, X$ processes, computed according to Eqs (6)–(8) of the text. Only the Sivers effect contributes. The computation is performed adopting the Sivers functions of Ref. [20] (SIDIS 1, left panel) and of Ref. [21] (SIDIS 2, right panel). The overall statistical uncertainty band, also shown, is the envelope of the two independent statistical uncertainty bands obtained following the procedure described in Appendix A of Ref. [21].

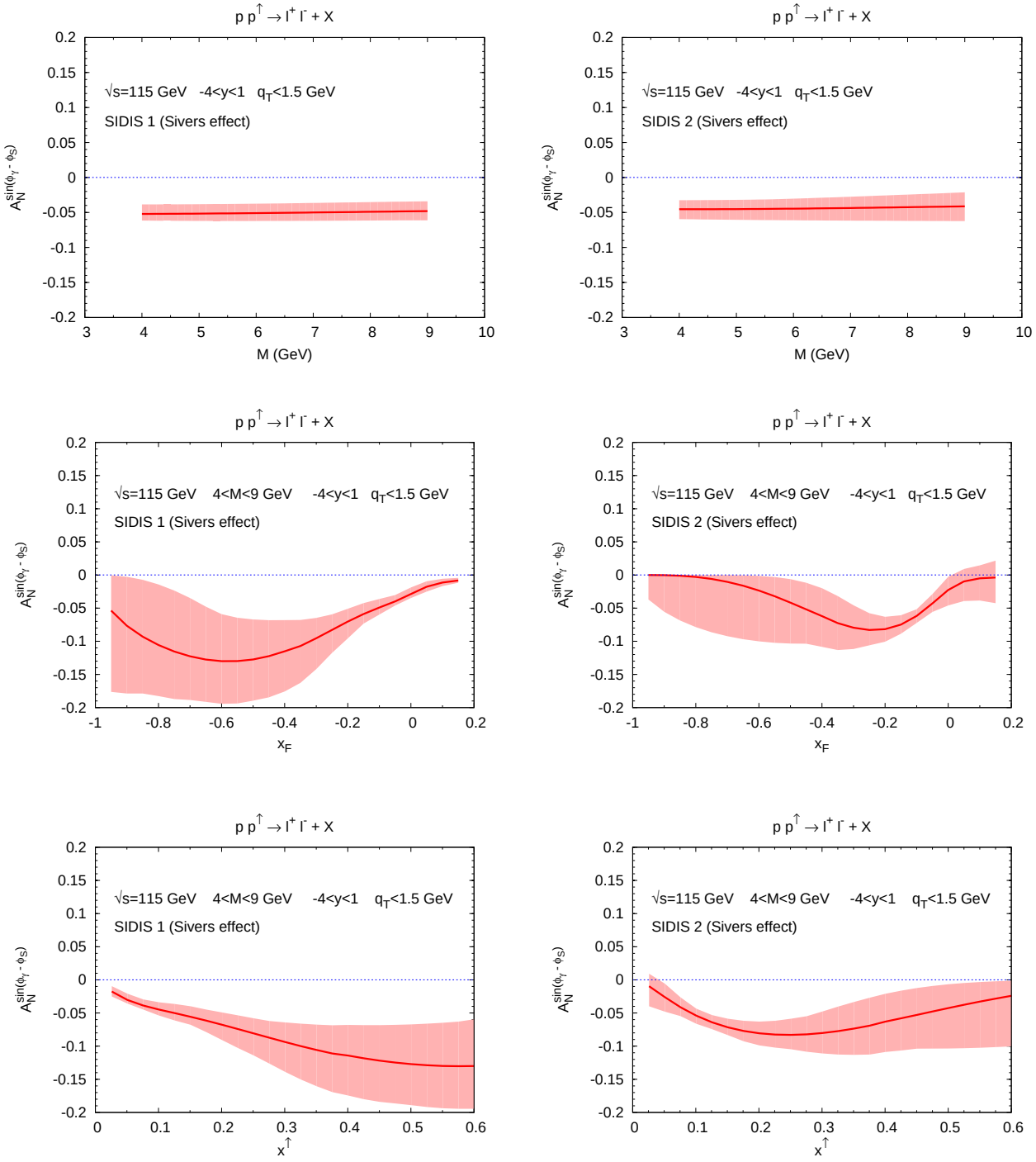

FIG. 10: Our theoretical estimates for $A_N^{(\phi_\gamma - \phi_S)}$ in D-Y processes as expected at AFTER@LHC. Our results are presented as function of M (upper plots), x_F (middle plots) and x of the quark inside the polarised proton, $x^\uparrow$ (lower plots). The other kinematical variables are either fixed or integrated, as indicated in each figure. They are computed according to Ref [35] and Eq. (23), adopting the Sivers functions of Ref. [20] (SIDIS 1, left panels) and of Ref. [21] (SIDIS 2, right panels), *reversed in sign*. The overall statistical uncertainty band, also shown, is obtained following the procedure described in Appendix A of Ref. [21].

[1] M. Anselmino, M. Boglione, U. D'Alesio, E. Leader, S. Melis, F. Murgia and A. Prokudin, Phys. Rev. **D86**, 074032 (2012), arXiv:1207.6529.
[2] M. Anselmino, M. Boglione, U. D'Alesio, S. Melis, F. Murgia and A. Prokudin, Phys. Rev. **D88**, 054023 (2013), arXiv:1304.7691.
[3] K. Kanazawa, Y. Koike, A. Metz, and D. Pitonyak, Phys. Rev. **D91**, 014013 (2015), arXiv:1410.3448.
[4] K. Kanazawa, Y. Koike, A. Metz, and D. Pitonyak, Phys. Rev. **D89**, 111501 (2014), arXiv:1404.1033.
[5] J.-w. Qiu and G. F. Sterman, Nucl. Phys. **B378**, 52 (1992).
[6] J.-w. Qiu and G. F. Sterman, Phys. Rev. **D59**, 014004 (1999), arXiv:hep-ph/9806356.
[7] C. Kouvaris, J.-W. Qiu, W. Vogelsang, and F. Yuan, Phys. Rev. **D74**, 114013 (2006), arXiv:hep-ph/0609238.
[8] X. Ji, J.-w. Qiu, W. Vogelsang, and F. Yuan, Phys. Rev. **D73**, 094017 (2006), arXiv:hep-ph/0604023.
[9] U. D'Alesio and F. Murgia, Prog. Part. Nucl. Phys. **61**, 394 (2008), arXiv:0712.4328.
[10] K. Kanazawa, Y. Koike, A. Metz, and D. Pitonyak, Adv. High Energy Phys. **2015**, 257934 (2015), arXiv:1502.04021.
[11] S. Brodsky, F. Fleuret, C. Hadjidakis, and J. Lansberg, Phys. Rept. **522**, 239 (2013), arXiv:1202.6585.
[12] L. Massacrier *et al.*, (2015), arXiv:1502.00984.
[13] D. W. Sivers, Phys. Rev. **D41**, 83 (1990).
[14] D. W. Sivers, Phys. Rev. **D43**, 261 (1991).
[15] J. C. Collins, Nucl. Phys. **B396**, 161 (1993).
[16] M. Anselmino, M. Boglione, U. D'Alesio, E. Leader, S. Melis and F. Murgia, Phys. Rev. **D73**, 014020 (2006), arXiv:hep-ph/0509035.
[17] P. J. Mulders and R. D. Tangerman, Nucl. Phys. **B461**, 197 (1996).
[18] A. Bacchetta, U. D'Alesio, M. Diehl, and C. A. Miller, Phys. Rev. **D70**, 117504 (2004), hep-ph/0410050.
[19] M. Anselmino, M. Boglione, U. D'Alesio, E. Leader, and F. Murgia, Phys. Rev. **D71**, 014002 (2005), hep-ph/0408356.
[20] M. Anselmino, M. Boglione, U. D'Alesio, A. Kotzinian, F. Murgia and A. Prokudin, Phys. Rev. **D72**, 094007 (2005), hep-ph/0507181.
[21] M. Anselmino, M. Boglione, U. D'Alesio, A. Kotzinian, S. Melis, F. Murgia, A. Prokudin and C. Türk, Eur. Phys. J. **A39**, 89 (2009), arXiv:0805.2677.
[22] M. Anselmino, M. Boglione, U. D'Alesio, A. Kotzinian, F. Murgia, A. Prokudin and C. Türk, Phys. Rev. **D75**, 054032 (2007), arXiv:hep-ph/0701006.
[23] M. Anselmino, M. Boglione, U. D'Alesio, A. Kotzinian, F. Murgia, A. Prokudin and S. Melis, Nucl. Phys. Proc. Suppl. **191**, 98 (2009), arXiv:0812.4366.
[24] M. Anselmino, U. D'Alesio, S. Melis, and F. Murgia, Phys. Rev. **D74**, 094011 (2006), arXiv:hep-ph/0608211.
[25] M. Gluck, E. Reya, and A. Vogt, Eur. Phys. J. **C5**, 461 (1998), hep-ph/9806404.
[26] D. de Florian, R. Sassot, and M. Stratmann, Phys. Rev. **D75**, 114010 (2007), arXiv:hep-ph/0703242.
[27] S. Kretzer, Phys. Rev. **D62**, 054001 (2000), arXiv:hep-ph/0003177.
[28] U. D'Alesio and F. Murgia, Phys. Rev. **D70**, 074009 (2004), arXiv:hep-ph/0408092.
[29] J. C. Collins, D. E. Soper, and G. F. Sterman, Nucl. Phys. **B250**, 199 (1985).
[30] X.-d. Ji, J.-P. Ma, and F. Yuan, Phys. Lett. **B597**, 299 (2004), arXiv:hep-ph/0405085.
[31] J. Collins, Foundations of perturbative QCD, Cambridge monographs on particle physics, nuclear physics and cosmology, N. 32, Cambridge University Press, Cambridge (2011).
[32] M. G. Echevarria, A. Idilbi, and I. Scimemi, JHEP **1207**, 002 (2012), arXiv:1111.4996.
[33] S. J. Brodsky, D. S. Hwang, and I. Schmidt, Phys. Lett. **B530**, 99 (2002), hep-ph/0201296.
[34] J. C. Collins, Phys. Lett. **B536**, 43 (2002), hep-ph/0204004.
[35] M. Anselmino, M. Boglione, U. D'Alesio, S. Melis, F. Murgia and A. Prokudin, Phys. Rev. **D79**, 054010 (2009), arXiv:0901.3078.